COMBUSTION STABILITY OF A HOMOGENEOUS MIXTURE IN A CHAMBER LINED WITH ACOUSTIC ABSORBERS

V. E. Doroshenko and V. M. Sil'verstov

UDC 534.28:536.46

Self-excited oscillations in cylindrical combustion chambers burning a homogeneous mixture are investigated theoretically and experimentally. It is shown that two low-order tangential-longitudinal modes differing slightly in frequency are excited in the model chamber. Judging from the closeness of the experimental and theoretical values obtained for the mass flow rate of the mixture at the self-excitation boundary, it is postulated that excitation is due to the dependence of chemical reaction rate on the pressure (temperature) of the medium.

The procedure used in the present study to analyze the high-frequency instability of the combustion process is based on the results of combustor model experiments [1] and involves small-scale model combustion chambers operating with a homogeneous gasoline–air mixture. Unstable combustion was investigated experimentally and theoretically in a chamber having cylindrical walls lined with acoustic absorbers.* The absorber effectiveness was assessed in the experiments on the basis of the acoustic self-excitation boundary plotted in the plane of the fuel-injection parameters, "percentage air excess versus mass flow rate of the mixture." The boundary separates the plane into domains of stable and unstable combustion. The most effective absorber is judged to be the one that minimizes the unstable combustion domain.

The model chamber (see the schematic diagram in Fig. 1a) includes a water-cooled nozzle 5 and water-cooled cylindrical sections 1. One of the sections is lined with an acoustic absorber 2, the length of which can be varied by means of heat-resistant spacers 6. This particular model makes it possible to preclude the influence of the cooling air for the absorbers on the unstable combustion boundary. The flame is maintained behind two V-shaped annular stabilizers 7, blocking off 70% of the chamber cross section. The temperature in the absorber cavity was measured with a Chromel–Alumel thermocouple 3, and the pressure oscillations in the chamber by means of three water-cooled tensometers 4 placed in the same cross section at a 90° angle relative to one another. The tests were conducted on model chambers with air cooling of the absorber. The air inlet line in this case is partitioned off from the absorber section by clusters of grids mounted in 16 connecting pipes spaced uniformly over the circumference. The absorber length (L_e) and distance from the absorber to the edge of the stabilizer (l_e) were varied between the following limits: $0 \leq L_e \leq 138$ mm; 30 mm $\leq l_e \leq 240$ mm.

The principal geometrical parameters of the acoustic absorber include the permeability σ (ratio of the single-perforation area to the surface area associated with one perforation), the perforation diameter d_0, the thickness t_e of the absorber walls, and the distance h_e between the absorber and the casing wall of the chamber. Constant values of $h_e = 10$ mm and $t_e = 1$ mm were used in all the experiments. The experimental absorbers had the following parameters: I) $d_0 = 2$ mm, $\sigma = 0.03$; II) $d_0 = 4$ mm, $\sigma = 0.03$; III) $d_0 = 6$ mm, $\sigma = 0.03$; IV) $d_0 = 8$ mm, $\sigma = 0.05$; V) $d_0 = 4$ mm, $\sigma = 0.01$; VI) $d_0 = 10$ mm, $\sigma = 0.05$.

*Inasmuch as the excitation of pressure oscillations in full-scale combustors for liquid-fuel rocket engines and gas turbine engines has a destructive effect on the combustor components, any prolonged oscillation, even of relatively small amplitude, cannot be tolerated. It was decided, therefore, to assess the instability of the combustion process and the effectiveness of methods for its abatement on the self-excitation boundary.

Moscow. Translated from Zhurnal Prikladnoi Mekhaniki i Tekhnicheskoi Fiziki, No. 1, pp. 76-82, January-February, 1975. Original article submitted June 26, 1974.

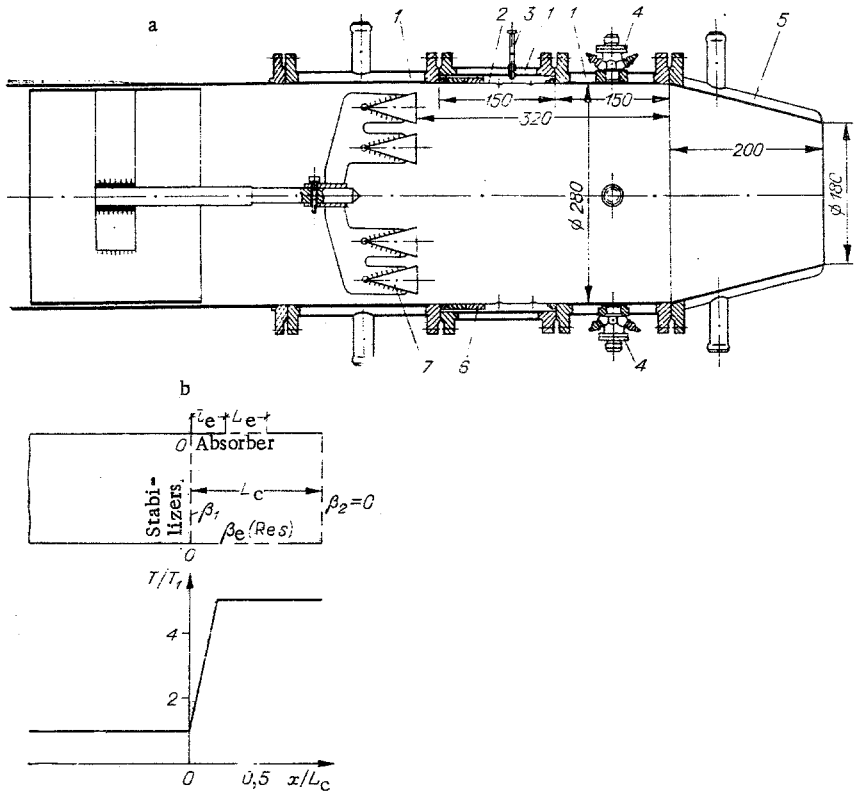

Fig. 1

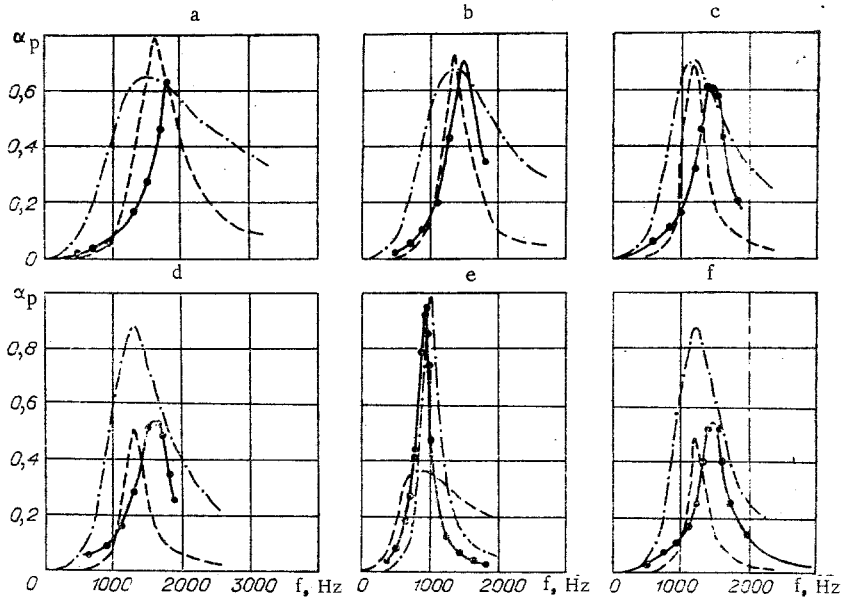

Fig. 2

The frequency response, i.e., the dependence of the absorption coefficient (ratio of the absorbed energy to the wave energy at normal incidence on the absorber surface) on the oscillation frequency, was determined experimentally (using the procedure and apparatus of Bruel and Kjaer A/S) and analytically (by the method of Blackman [2]) for each of the absorbers. The frequency responses of absorbers I-VI are given in Fig. 2a-f, respectively. The acoustic frequency f is plotted on the horizontal, and the absorption coefficient α_p on the vertical, axis. The curves and dots give the results of the calculations under the measurement conditions, and the dot-dashed curves give the results of the calculations under flame-test conditions (acoustic intensity level 180 dB; pressure 147.5 k Pa; temperature 293°K). The values of the

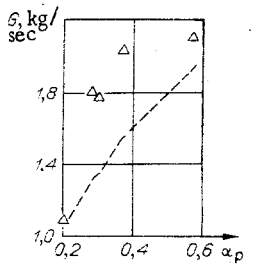

Fig. 3

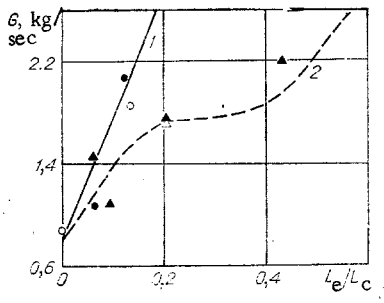

Fig. 4

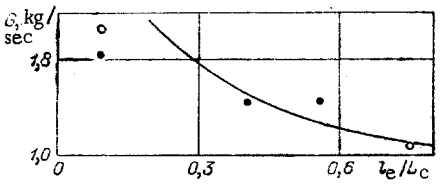

Fig. 5

absorption coefficient at an acoustic level of 110 dB are close to the corresponding experimental values, a slight disparity in the resonance frequency being attributable to the choice of end correction [2]. The flame-test absorption coefficient depends on certain parameters disregarded in the calculations and measurements, such as the cross-flow of gas through the absorber perforations and the slip-flow velocity along the surface. The resulting frequency curves nonetheless afford a qualitative assessment of the acoustical properties of the absorbers.

In the flame tests, tangential-longitudinal modes were observed with frequencies of 1.9 to 2.3 kHz and 1.6 to 1.8 kHz. The second mode is excited in regimes with frequencies of 1.9 to 2.3 kHz, while the oscillations at 1.6 to 1.8 kHz must be associated with the first tangential-longitudinal mode (in the classification of Sil'verstov [3]).

The experimental investigation made it possible to assess the influence of the follower parameters on the unstable combustion boundary: the energy absorption coefficient α_p calculated at 2 kHz (which is the average frequency of the oscillations excited in the cavity); the absorber length L_e; and the absorber position l_e.

The experimental results were used to plot the curves in Figs. 3-5. The vertical coordinate represents the mixture flow rates G at which high-frequency oscillations are excited, and the horizontal represents the values of the absorption coefficient (Fig. 3), relative absorber length L_e/L_c (Fig. 4), and relative distance l_e/L_c from the stabilizers (Fig. 5). The experimental results for the chamber without air cross-flow through the absorber are indicated by dark symbols, and those for the chamber with air cooling, by light symbols. The circles correspond to points for the first oscillatory mode and the triangles, to points for the second mode. The points correspond to a near-stoichiometric composition of the mixture ($\alpha_\Sigma = 0.95$ to 1.07), i.e., to the typical operating regime of combustors for liquid-fuel rocket engines and gas turbine engines. The analogous curves for other values of the air excess are not given here.

The velocity in the absorber perforations for the cross-flow model varied only slightly (V = 60 to 80 m/sec).

In determining the influence of α_p, absorbers of equal length ($L_e = 138$ mm; $L_e/L_c = 0.43$) were installed in the combustion chamber in an identical setting ($l_e = 30$; $l_e/L_c = 0.093$). The influence of the length and position was investigated in chambers with absorber II ($d_0 = 2$ mm; $\sigma = 0.03$; $\alpha_p = 0.68$). For a variable absorber position the length was held constant ($L_e = 41$ mm; $L_e/L_c = 0.13$), and for a variable length the distance from the absorber to the edge of the stabilizers was held constant ($l_e = 30$ mm; $l_e/L_c = 0.093$).

The experiments showed that: 1) the stability of the combustion process is greatly enhanced by increasing the absorption coefficient (Fig. 3) and length of the acoustic absorber (Fig. 4); 2) the maximum stability in the model chamber is provided by an absorber situated close to the stabilizers; 3) the stability deteriorates as the distance of the absorber from the stabilizers is increased (Fig. 5).

We now carry out a theoretical analysis of the self-excitation of acoustic oscillations for an inviscid nonthermally conducting gas described by the system of equations

$$\frac{1}{\varkappa P}\frac{dP}{dt} + \operatorname{div}\mathbf{V} = \frac{\varkappa - 1}{\varkappa}\frac{qW}{P};$$

$$\frac{d\mathbf{V}}{dt} + \frac{\nabla P}{\rho} = 0;\quad \frac{1}{\rho}\frac{d\rho}{dt} + \operatorname{div}\mathbf{V} = 0;$$

$$P = (\varkappa - 1)c_v T\rho = \rho RT.$$

Here ρ, P, T, $\mathbf{V}$, and W are the density, pressure, temperature, flow velocity of the gas, and chemical reaction rate; $\varkappa$ is the adiabatic exponent; and q is the heating capacity of the fuel.

We set $P = P_0 + p'$; $\rho = \rho_0 + \rho'$; $T = T_0 + T'$; $\mathbf{V} = \mathbf{V}_0 + \mathbf{v}'$; and $W = W_0 + w'$, where P_0, ρ_0, T_0, V_0, and W_0 are the parameters of the unperturbed state ($\mathbf{V}_0$ is directed along the x axis) and p', ρ', T', $\mathbf{v}'$, and w' are small unsteady perturbations of the corresponding parameters.

From the steady-flow gasdynamical equations we obtain relations between the gradients of the average variables and the gradient of the cross-sectional average temperature of the gas in the chamber:

$$\frac{\partial P_0}{\partial x} = -\frac{M^2 \varkappa P_0}{(1-\varkappa M^2)} \frac{1}{T_0} \frac{\partial T_0}{\partial x};$$
$$\frac{\partial \rho_0}{\partial x} = -\frac{\rho_0}{(1-\varkappa M^2)} \frac{1}{T_0} \frac{\partial T_0}{\partial x}; \tag{1}$$
$$\frac{\partial V_0}{\partial x} = \frac{M}{(1-\varkappa M^2)} \sqrt{T_0 (\varkappa - 1) c_v} \frac{1}{T_0} \frac{\partial T_0}{\partial x} = \frac{\varkappa - 1}{\varkappa (1 - M^2)} q \frac{W_0}{P_0}.$$

where M is the cross-sectional average Mach number.

The linearized system of equations for the airstream parameters, taking (1) into account, is written in the form

$$\frac{1}{\varkappa P_0} \frac{\partial p'}{\partial t} + \frac{\partial v_x'}{\partial x} + \frac{\partial v_y'}{\partial y} + \frac{\partial v_z'}{\partial z} + \frac{V_0}{\varkappa P_0} \frac{\partial p'}{\partial x} - \frac{M(n-1)}{T_0 P_0} \sqrt{(\varkappa - 1) c_v T_0 \varkappa} \frac{dT_0}{dx} p' = 0;$$
$$\rho_0 \frac{\partial v_x'}{\partial t} + V_0 \rho_0 \frac{\partial v_x'}{\partial x} + \frac{\partial p'}{\partial x} = 0;$$
$$\rho_0 \frac{\partial v_y'}{\partial t} + V_0 \rho_0 \frac{\partial v_y'}{\partial x} + \frac{\partial p'}{\partial y} = 0; \tag{2}$$
$$\rho_0 \frac{\partial v_z'}{\partial t} + V_0 \rho_0 \frac{\partial v_z'}{\partial x} + \frac{\partial p'}{\partial z} = 0.$$

The interaction ratio $n = w'/W_0 \,|\, p'/P_0$ gives the relationship between the relative perturbations of the chemical reaction rate and pressure [4]. The so-called energy integral identity holds for systems of this type [4]; for a piecewise-smooth surface S bounding a four-dimensional domain g situated inside the domain of existence of the solution, it has the form

$$\frac{1}{2} \oint_S \left\{ \left[\frac{p'^2}{2\varkappa P_0} + \rho_0 \left(v_x'^2 + v_y'^2 + v_z'^2 \right) \right] \tau + \left[V_0 \left(\frac{p'^2}{\varkappa P_0} + \rho_0 \left(v_x'^2 + \right. \right. \right.$$
$$\left. \left. \left. + v_y'^2 + v_z'^2 \right) \right) \right] \xi + [2p' (\mathbf{v}\mathbf{n})] \right\} dS = \frac{1}{2} \int\int\int\int_g \left\{ \left[\frac{V_0}{T_0} \frac{dT_0}{dx} n \frac{p'^2}{P_0} \right] + \right.$$
$$\left. + \left[\frac{dV_0}{dx} \left((2\varkappa - 1) \frac{p'^2}{\varkappa P_0} + 2\rho v_x'^2 \right) \right] \right\} dx\, dy\, dz\, dt, \tag{3}$$

where (τ, ξ, η, ζ) is the unit outward normal vector to S, and $\mathbf{n}$ is the normal vector in three-dimensional space.

The first bracketed term on the left-hand side of Eq. (3) corresponds to the energy variation in the volume of the cylindrical cavity in the time interval $(t_2 - t_1)$, where $t = t_1$ and $t = t_2$ are the hyperplanes bounding the domain g. The second term corresponds to the energy influx due to the average motion in the time $(t_2 - t_1)$ through the end surfaces, perpendicular to the x axis, of the cylindrical cavity. Finally, the last term corresponds to the loss of acoustic energy through the lateral surfaces of the cylinder in the time $(t_2 - t_1)$ as a result of, for example, the flow of energy toward the absorber.

The first term on the right-hand side of Eq. (3) corresponds to the increase in acoustic potential energy in the volume due to fluctuating heat release. In the absence of fluctuating heat release ($n = 0$) this energy increase is zero. The second term on the right-hand side corresponds to the loss of acoustic energy in the volume in the time $(t_2 - t_1)$ due to interaction of the accelerated flow with the acoustic oscillations ($dV_0/dt = V_0$, $dV_0/dx > 0$). The problem of interaction between the acoustic oscillations and average motion of the gas is important enough to merit separate investigation. We limit the present study to the generation of wave energy in the combustion zone and omit in the system of equations (2) terms associated with the average motion (without heat release), as well as terms governing interaction of the flow with acoustic oscillations in the presence of a net average heat release. Then, eliminating V, we obtain an equation for the propagation of sound in the section of the cavity with a variable temperature over the length, taking into account fluctuating heat release:

$$\frac{1}{[a(x)]^2} \frac{\partial^2 p'}{\partial t^2} - \frac{1}{T_0} \frac{dT_0}{dx} \frac{\partial p'}{\partial x} - \Delta p' = \mathrm{Ma} \frac{1}{T_0} \frac{dT_0}{dx} n \frac{1}{P_0} \frac{\partial p'}{\partial t}. \tag{4}$$

Equation (4) differs from the corresponding equation given in [3] by the inclusion of the fluctuating heat-release term on the right-hand side.

The problem is essentially to determine the complex frequency in a cylindrical cavity filled with a hot gas having a lengthwise-variable temperature. In the hot section the sound-propagation equation coincides with the usual wave equation.

The walls of the cavity without the absorbers are assumed to be absolutely acoustically rigid, and the impedance of the surface of the absorber-lined section is considered to be homogeneous and dependent on the frequency (Res). Each section is partitioned into three parts, two without absorbers and one in between with an absorber. The solutions for each part are sought in cylindrical coordinates (x, r, φ) in series form on the assumption that the dependence of the solutions on the angle φ is the same for all parts. In the junction cross sections (common to two parts) the solutions are joined so that the oscillatory pressures and axial velocities are equal there. It is assumed in the calculations that the junction conditions are satisfied at a finite number of values of the radius, and the expressions for the solutions in each part are limited to a finite number of terms. The junction conditions and boundary conditions enable us, in making the successive transition from one part to the next, to derive relations by which the complex frequency (s) of the oscillations can be calculated as in [3]. When acoustic energy losses are present, the oscillations generated by zonal combustion can grow (Im s > 0), decay (Im s < 0), or remain unchanged (Im s = 0), depending on the values of the fuel-injection parameters. The self-excitation boundaries are plotted according to the condition that Ims is equal to zero at the boundary.

As is apparent from the right-hand side of Eq. (3), oscillations are self-excited mainly by fluctuating heat release in the vicinity of the maximum pressure oscillation amplitudes. For the investigated lowest tangential-longitudinal modes the pressure amplitude is a maximum at the cylindrical wall and a minimum on the axis. In the experimental chamber the length of the combustion is smaller at the wall than on the axis. It is assumed in the calculations, therefore, that the gradient of the cross-sectional average temperature of the gas coincides in the entire cavity with the temperature gradient at the cylindrical wall (see Fig. 1b). The length of the temperature-gradient section is determined by the angle of inclination of the flame front stabilized behind the flow-obstructing body. According to the data of [5], this angle is 7 to 9°. Consequently, for a space of 10 mm between the edge of the outer stabilizer and the cylindrical chamber wall it may be assumed that the variable-temperature section takes up a fifth of the chamber, while the rest is filled with hot gas (see Fig. 1b).

We have calculated the mixture flow rate at the self-excitation boundary for both the first and second modes as a function of the length of different absorbers for a fixed air excess ($\alpha_\Sigma = 1$). We assume that a traveling wave propagates upstream from the stabilizers, i.e., the acoustic admittance at the chamber entry (in the stabilizer cross section) is equal to -1 ($\beta_1 = -1$). The loss of acoustic energy through the nozzle is neglected ($\beta_2 = 0$). The interaction ratio n is chosen so that the mass flow rate of the mixture at the self-excitation boundary in the combustion chamber without absorbers will be close to the experimental value (with $\alpha_\Sigma = 1$) for the model combustion chamber without absorbers ($G \cong 0.8$ kg/sec); the value of n is close to that calculated in [6]. We have $n = 2.4$ for the first mode and $n = 3$ for the second mode.

The dashed curve in Fig. 4 represents the theoretical self-excitation boundary for the second mode with $n = 3$, and the solid curve represents the same for the first mode with $n = 2.4$.

The experimental points for both the first and the second mode are close to the corresponding theoretical curves.

The dashed curve in Fig. 3 represents the theoretical values obtained for the second mode with a relative absorber length $L_e/L_c = 0.43$.

The theoretical curves for the mixture flow rate at the self-excitation boundary for the second mode are consistent with the experimental values.

The solid curve in Fig. 5 represents the analytical results for the first mode. The length of the absorber is the same in the calculations as in the experiment ($L_e = 40$ mm; $L_e/L_c = 0.13$).

The experimental points are reasonably close to the theoretical curve for the first mode. The deviations at large values of the mixture flow rate can be attributed to the fact that the influence of the air flow rate on the length of the combustion zone is neglected in the calculations. Thus, the theory provides a qualitatively correct description of the experimental data on the influence of absorbers.

LITERATURE CITED

1. V. E. Doroshenko, S. F. Zaitsev, and V. I. Furletov, "Two operating regimes of a model combustion chamber as a self-excited thermoacoustic system," Zh. Prikl. Mekhan. i Tekh. Fiz., No. 1 (1967).
2. A. W. Blackman, "Effect of nonlinear losses on the design of absorbers for combustion instabilities," ARS Journal, 30, No. 11 (1960).
3. V. M. Sil'verstov, "Lowest tangential-longitudinal modes in a closed cylindrical cavity filled with a variable-temperature gas," Akust. Zh., 20, No. 2 (1974).
4. S. K. Godunov, Equations of Mathematical Physics [in Russian], Nauka, Moscow (1971).
5. B. V. Raushenbakh, S. A. Belyi, I. V. Bespalov, V. Ya. Borodachev, M. S.Volynskii, and A. G. Prudnikov, Physical Foundations of the Working Process in Air-Breathing Jet Engines [in Russian], Mashinostroenie, Moscow (1964).
6. V. I. Furletov and V. A. Sklyarov, "Frequency response of a laminar flame," Zh. Prikl. Mekhan. i Tekh. Fiz., No. 1 (1974).